Magnetic order and spin dynamics in the proximity of a ferromagnetic quantum critical point: A μSR study of YbNi$_4$P$_2$

J. Spehling,[1] M. Günther,[1] C. Krellner,[2,3] N. Yèche,[1] H. Luetkens,[4] C. Baines,[4] C. Geibel,[2] and H.-H. Klauss[1,*]

[1]*Institute for Solid State Physics, TU Dresden, D-01069 Dresden, Germany*

[2]*Max Planck Institute for Chemical Physics of Solids, D-01187 Dresden, Germany*

[3]*Cavendish Laboratory, University of Cambridge, J. J. Thomson Avenue, Cambridge CB3 0HE, United Kingdom*

[4]*Laboratory for Muon-Spin Spectroscopy, Paul-Scherrer-Institute, CH-5232 Villigen, Switzerland*

The local $4f$-electronic spin dynamics and magnetic order in YbNi$_4$P$_2$ were studied by means of muon-spin relaxation measurements. Zero-field muon-spin relaxation proves static magnetic order with a strongly reduced ordered Yb^{3+} moment of $(2.5-4.6) \times 10^{-2} \mu_B$, below $T_C = 140$ mK. Above T_C, the muon-spin polarization $P(t,B)$ is dominated by quasihomogeneous spin fluctuations and exhibits a time-field scaling relation $P(t,B) = P(t/B^\gamma)$, indicating cooperative critical spin dynamics in the system. At $T = 190$ mK, slightly above T_C, $\gamma = 0.81(5)$, suggesting time-scale invariant power-law behavior for the dynamic electronic spin-spin autocorrelation function.

Lanthanide-based heavy-fermion (HF) systems are suitable model systems to study emergent phenomena at a quantum critical point (QCP), where collective quantum fluctuations trigger the system continuously from a magnetically ordered to a nonmagnetic ground state.[1–6] However, despite intense research, to the best of our knowledge, no $4f$-based material is known with a continuous ferromagnetic (FM) to paramagnetic (PM) quantum phase transition (QPT). The existence of such a QPT is also controversially discussed from a theoretical point of view.[7–11]

Recently, Krellner *et al.* suggested that the HF metal YbNi$_4$P$_2$ with a quasi-one-dimensional (1D) electronic structure exhibits FM quantum criticality above a low FM transition temperature $T_C = 170$ mK.[12] YbNi$_4$P$_2$ crystallizes in the tetragonal ZrFe$_4$Si$_2$ structure containing isolated chains of edge-connected Ni tetrahedra along the c axis. The Yb atoms are located in the channels between these Ni tetrahedral chains. The reduced dimensionality in the Yb and Ni network and the geometrical frustration between neighboring Yb chains give rise to enhanced quantum spin fluctuations of the magnetic Yb^{3+} ions. In the PM state above 50 K, the magnetic susceptibility shows Curie-Weiss behavior with an effective moment $\mu_{\rm eff} = 4.52 \mu_B$ that is characteristic for magnetic Yb^{3+} ions. Analysis of the magnetic entropy reveals a Kondo energy scale of $T_K \approx 8$ K for the crystal electric field ground-state doublet. The FM transition is evidenced by distinct anomalies in magnetic susceptibility, specific heat, and resistivity measurements. Low-T magnetization measurements suggest an ordered FM moment of $m_{\rm ord} \approx 0.05(4) \mu_B$. Pronounced non-Fermi-liquid (NFL) behavior is reflected by a stronger-than-logarithmic diverging Sommerfeld coefficient and a linear-in-T resistivity state apparent in a T range larger than a decade above T_C. In external magnetic fields, the NFL behavior is suppressed and FL behavior gradually recovers. Therefore, YbNi$_4$P$_2$ is considered as a clean system situated in the very close vicinity of a FM QCP, with FM quantum fluctuations dominating thermodynamic and transport quantities at $T > T_C$.

The present knowledge on YbNi$_4$P$_2$ is based on measurements of macroscopic magnetic, thermodynamic, and transport properties. The next step in a deeper investigation of this prospective FM quantum critical system is to get insight on a microscopic level. Besides the nature of the magnetic order, a central issue in the present context of critical behavior is the spin dynamics. Since in systems close to a QCP, the ordered moment is usually strongly reduced, muon-spin relaxation (μSR) has proven to be an extremely valuable technique to collect appropriate information.[13–15]

Here, we present μSR experiments on polycrystalline YbNi$_4$P$_2$, providing microscopic evidence for static magnetism at $T \leqslant T_C \approx 140$ mK with an ordered moment of $m_{\rm ord} = (2.5-4.6) \times 10^{-2} \mu_B$/Yb, depending on the assumed muon site. Above T_C, the muon-spin polarization $P(t)$ obeys the time-field scaling relation $P(t) = P(t/B^{0.81(5)})$, indicating cooperative and critical spin dynamics.

In a μSR experiment positive spin-polarized muons are implanted into the sample, and the subsequent time evolution of the muon-spin polarization is monitored by detecting the asymmetric spatial distribution of positrons emitted from the muon decay.[16] μSR in longitudinal applied magnetic fields is dominated by Yb-$4f$ electronic spin fluctuations that couple to the implanted muons. The μSR experiments on YbNi$_4$P$_2$ in zero field (ZF) and longitudinal (LF) applied field—with respect to the initial muon spin polarization—were performed on the πM3 beam line at the Swiss Muon Source at the Paul-Scherrer-Institut, Switzerland. The sample was prepared by crushing $\sim$270 mg of single-crystalline material, grown in a self-flux at 1400 °C in a closed Tantal crucible, and characterized by powder x-ray diffraction experiments, proving the absence of any foreign phases. Detailed low-T measurements on polycrystalline YbNi$_4$P$_2$ were reported elsewhere.[12]

Figure 1(a) displays typical time dependencies of the ZF muon-spin polarization $P(t)$ in YbNi$_4$P$_2$ at representative temperatures above and below T_C. A finite T-independent background signal due to muons that stopped in a Ag sample holder (signal fraction $\approx$50%) was taken into account. At $T \geqslant 160$ mK, an exponential muon-spin relaxation is
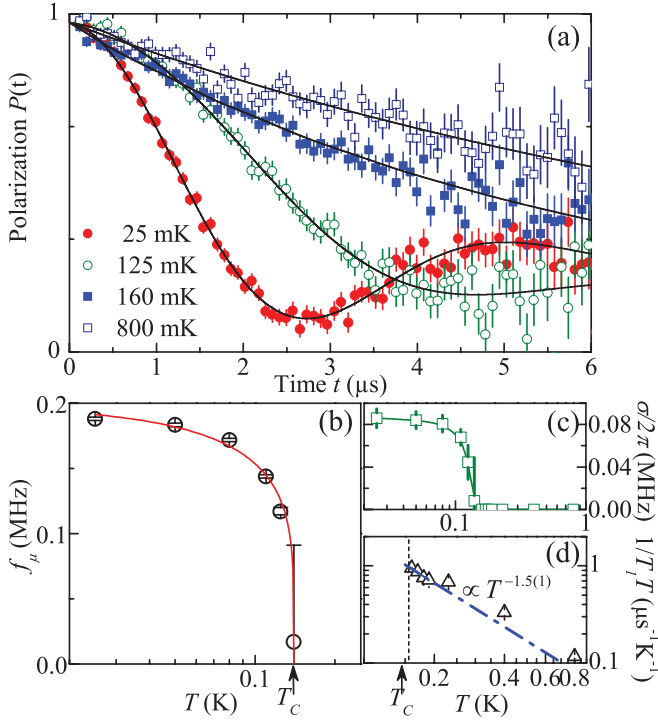
FIG. 1. (Color online) (a) Corrected muon-spin polarization $P(t)$ at ZF for representative T above and below $T_C \approx 140$ mK. At $T \leqslant T_C$, solid lines are fitting curves according to Eq. (1). (b) T dependence of the ZF μSR frequency $f_\mu(T)$. The solid line is a fit to the phenomenological function $f_\mu = f_\mu(0)(1 - \frac{T}{T_C})^n$. (c) T dependence of the ZF static internal field distribution σ in Eq. (1). The solid line is a guide to the eye. (d) T dependence of $1/T_1 T$ in the PM regime. The line describes power-law behavior as $\frac{1}{T_1 T} \propto T^{-1.5}$.

associated with fast fluctuating paramagnetic electron spins with a relaxation rate $\lambda(160 \text{ mK}) \approx 0.152(2) \ \mu\text{s}^{-1}$. Note that dense static nuclear dipole moments would give rise to a weak Gaussian relaxation in the PM regime. While cooling through T_C, an additional magnetic relaxation mechanism is apparent, strongly increasing with lowering T. Below T_C, a low-frequency oscillation with a Gaussian relaxation of the muon-spin polarization is observed, indicating magnetic ordering of weak electronic Yb^{3+} moments. The muon-spin asymmetry data in the FM regime can be described best using the functional form[17,18]

$$P(t) = \frac{1}{3} + \frac{2}{3}\left[\cos(2\pi f_\mu t) - \frac{\sigma^2 t}{2\pi f_\mu}\sin(2\pi f_\mu t)\right]e^{-\frac{1}{2}\sigma^2 t^2},$$

(1)

where f_μ and σ are the muon-spin precession frequency and the Gaussian field width, respectively. The 2/3 oscillating and the 1/3 nonoscillating terms originate from the spatial averaging in polycrystalline samples, where 2/3 (1/3) of the internal magnetic field components are directed perpendicular (parallel) to the initial muon spin, causing a precession (no precession) of the muon spin. The observation of a 2/3 and 1/3 signal fraction below T_C implies dense magnetic moments and proof that 100% of the sample volume shows static magnetic order. The latter is supported by LF-μSR measurements, as discussed in detail below. In the limit $2\pi f_\mu \gg \sigma$, Eq. (1)

becomes a Gaussian damped cosine function. For $2\pi f_\mu \to 0$, close to the magnetic transition, Eq. (1) is equivalent to the Gaussian Kubo-Toyabe (GKT) function,[19] which describes a muon-spin relaxation due to a static Gaussian field distribution centered around $B_{\text{local}} = 0$. ZF-μSR on the antiferromagnetically ordered system $YbRh_2Si_2$ (Ref. 14) reveals a similar crossover from a Lorentzian to a Gaussian damped μSR signal in the vicinity of the PM to magnetic phase transition, attributed to a transition from dynamic to static magnetism of magnetic Yb^{3+} moments.

For $YbNi_4P_2$ a finite μSR frequency is clearly observed below 150 mK. From the measured frequency value $f_\mu = 0.188(1)$ MHz at 20 mK one can determine the internal local field at the muon site to $B_{\text{local}} = 13.87$ G using $B_{\text{local}} = 2\pi f_\mu/\gamma_\mu$, with $\gamma_\mu = 2\pi \times 13.55$ kHz/G as the muon gyromagnetic ratio. The local field B_{local} as well as the local static field width $\Delta B_{\text{local}} = \sigma/\gamma_\mu \approx 6$ G are very small for conventional rare-earth magnets with large ordered moments. The fractional width $\Delta B_{\text{local}}/B_{\text{local}}$ of the spontaneous field distribution is ~ 0.4 at low T and remains constant as $T \to T_C$, which is a reasonable value for a magnetically ordered HF system, as, e.g., in $CeRhIn_5$, $\Delta B_{\text{local}}/B_{\text{local}} = 0.5$ is observed.[20] Thus, the local field distribution is nearly uniform and homogeneous in the FM regime. The spontaneous muon-spin precession and the Gaussian shape of the internal field distribution below T_C arise from a dense system of weak magnetic moments with small, static magnetic inhomogeneities. The presence of a finite $B_{\text{local}} \neq 0$ proves coherent magnetic order.

ZF-μSR allows a precise determination of the T dependence of the magnetic order parameter, which is proportional to the measured μSR frequency f_μ. The T dependence of f_μ and σ is shown in Figs. 1(b) and 1(c). For $T \leqslant$ 140 mK, both observables exhibit a continuous increase. The T dependence of f_μ can be fit to the phenomenological function $f_\mu = f_\mu(0)(1 - \frac{T}{T_C})^n$ for $T < T_C$ with $n = 0.208 \pm 0.02$, $f_\mu(T) = 0.199(3)$ MHz, and $T_C = 140(2)$ mK. The value of the effective critical exponent n, describing the critical behavior close to T_C, is between $n = 0.125$ and 0.325, which are theoretically expected for two-dimensional (2D) and isotropic three-dimensional (3D) Ising magnets, respectively. This is not in contradiction with the claim of a quasi-1D system. In such a system, the weak interchain coupling results in an evolution from a 1D behavior at high T to a 2D Ising or 3D behavior at low T, which is intimately linked with (and is a prerequisite for) the long-range ordering at finite T. The low data point density between $0.6 \leqslant \frac{T}{T_C} \leqslant 1$, however, precludes the determination of the precise critical exponent. The obtained value for T_C agrees well with the value found in specific-heat measurements on these single crystals.[21]

For all examined $T \leqslant T_C$, the sample signal is analyzed with a well-defined single f_μ and σ, signaling that the magnetic order is a bulk effect and that only one dominant muon stopping site is present. In general, for the determination of the muon stopping site(s) it is important to deduce the hyperfine coupling constant. One way to find potential muon sites is to compare calculated and measured quantities for the local field B_{local} at the muon site. The muon preferentially settles at tetrahedra or octahedra interstitial crystallographic sites. From simple symmetry arguments the

most probable muon stopping sites, using Wyckoff's notation, are $4f(1/4,1/4,0)$, $8j(1/4,1/4,1/4)$, $4f(1/4,1/4,1/2)$, $8i(1/4,1/2,1/2)$, $4c(1/2,0,0)$, $4c(1/2,0,1/2)$, $2b(0,0,1/2)$, and $2a(1/2,1/2,1/2)$. For a particular FM structure with the magnetic Yb^{3+} moments aligned within the a-b plane and a dominant $4f$-μ dipolar interaction, one can determine the expected internal field values for the proposed sites. Our lattice sum calculations reveal that only at the $4c(1/2,0,1/2)$ site and $8i(1/4,1/2,1/2)$ site a local field B_{local} of the measured absolute magnitude is found. For the $4c$ and $8i$ sites the measured local field of $B_{\text{local}} = 13.87$ G corresponds to a static ordered moment of the Yb ions of $m_{\text{ord}} = 0.046\mu_B$ and $0.025\mu_B$, respectively. Both values are in good agreement with the value deduced from recent magnetization measurements.[12]

The temperature dependence of the exponential relaxation rate $\lambda_L = \frac{1}{T_1}$, observed above T_C, is plotted in Fig. 1(d) on a log-log scale as $\frac{1}{T_1T}$. Cooling down from 800 mK, $\frac{1}{T_1T}$ exhibits power-law behavior according to $\frac{1}{T_1T} \propto T^{-1.40(6)}$. At $T \leqslant 190$ mK, the power-law behavior in $\frac{1}{T_1T}$ persists in the PM regime down to T_C, however, with a slight change of the critical exponent, i.e., $\frac{1}{T_1T} \propto T^{-1.5(1)}$ (dashed-dotted line). The observed $\frac{1}{T_1T}$ behavior is close to the $T^{-4/3}$ temperature dependence predicted by the self-consistent renormalization (SCR) theory for a system close to a 3D ferromagnetic QCP.[22] There is no prediction for an itinerant quasi-1D system in the T range between the exchange energy scale and ordering temperature. For an isolating ferromagnetic quasi-1D spin chain the T dependence of the relaxation rate above T_C depends strongly on the details of the interactions—see, e.g., Ref. 23.

LF-μSR experiments allow to separate the dynamic contribution to the relaxation of the muon-spin polarization. Investigations of the low-T muon-spin dynamics yield additional information about the origin of the NFL behavior in $YbNi_4P_2$. Figure 2 displays the muon-spin asymmetry function $P(t)$ at $T = 20$ mK for different applied LFs. The muon-spin relaxation is completely suppressed in an applied field $B_{\text{LF}} \approx 300$ G, demonstrating that the internal field distribution is static in nature. However, the observed decoupling cannot be described accurately by a standard muon asymmetry function that considers an internal field distribution
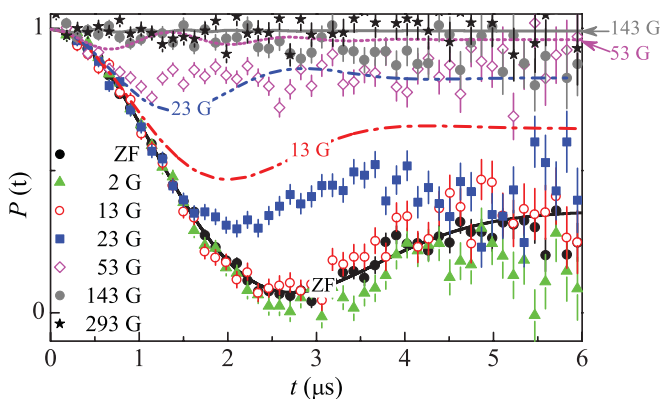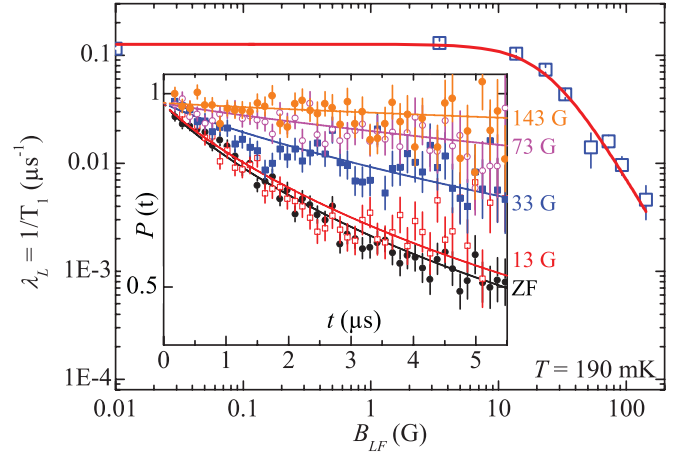

FIG. 3. (Color online) Main panel: Field dependence of the dynamic muon-spin relaxation rate λ_L. The solid curve represents a Redfield fit. For display reasons, the ZF value is set at $B_{\text{LF}} = 0.01$ G. Inset: Field dependence of the corrected muon-spin polarization $P(t)$ at $T = 190$ mK.

which is symmetric around $B_{\text{local}} = 0$. For comparison, Fig. 2 shows theoretical depolarization curves for the static GKT function in the corresponding longitudinal magnetic fields. This supports the ZF data, i.e., the observation of a broad field distribution centered around a finite but small internal field $B_{\text{local}}(20$ mK$) \approx 13.87$ G in the FM phase. Finally, when $B_{\text{LF}} \gg B_{\text{local}}$, the muon-spin relaxation is decoupled from the static B_{local} as observed for $B_{\text{LF}} \geqslant 23$ G.

At $T > T_C$, the field dependence of the muon-spin relaxation probes the Fourier transform of the dynamic spin-spin autocorrelation function $q(t) = \langle S_i(t) \cdot S_i(0) \rangle$, which exhibits exponential behavior for homogeneous systems and power-law (or cutoff power-law) or stretched exponential behavior for inhomogeneous systems. The inset of Fig. 3 displays the muon-spin polarization $P(t)$ at $T = 190$ mK, both in magnetic LF between 13 and 143 G and ZF. The relaxation rate λ_L is reduced with increasing field. The field dependence of λ_L is given in the main panel of Fig. 3. It shows nearly no field dependence for magnetic fields of less than $\sim$13 G, but varies more strongly, as $H^{-\kappa}$ with $\kappa \approx 0.79(7)$, for higher fields. From the field dependence of λ_L, the spin autocorrelation time τ_c can be estimated using the Redfield formalism for $\lambda_L(B_{\text{LF}}) = (2\gamma_\mu^2 \langle B_{\text{fluc}}^2 \rangle \tau_c)/[1 + (\gamma_\mu^2 B_{\text{LF}}^2 \tau_c^2)]$ considering τ_c as independent of the applied field B_{LF}. Here, $B_{\text{fluc}}(t)$ describes the time-varying local magnetic field at the muon site due to fluctuations of neighboring Yb^{3+} moments, with a local time-averaged second moment $\Delta^2 = \gamma_\mu^2 \langle B_{\text{fluc}}^2 \rangle$ and a single fluctuation time τ_c. For $\hbar\omega \ll k_B T$ (ω giving the spin fluctuation rate), the fluctuation-dissipation theorem[24] relates τ_c to the imaginary component of the local q-independent f-electron dynamic susceptibility, i.e., $\tau_c(B) = (k_B T)[\chi''(\omega)/\omega]$. The fit to the data (solid curve in the main panel of Fig. 3) yields $\Delta^2 \approx 0.1$ (MHz) and $\tau_c \approx 6 \times 10^{-7}$ s, the latter value nearly three orders of magnitude larger than the one obtained for $YbRh_2Si_2$ at $T = 20$ mK,[14] suggesting very slow critical fluctuations.

The μSR time spectra in Fig. 3 are well described with a stretched exponential relaxation function of the form

FIG. 2. (Color online) Corrected muon-spin polarization at $T = 20$ mK and various longitudinal magnetic fields B_{LF}. The lines represent theoretical depolarization curves for the static GKT function in corresponding longitudinal fields.
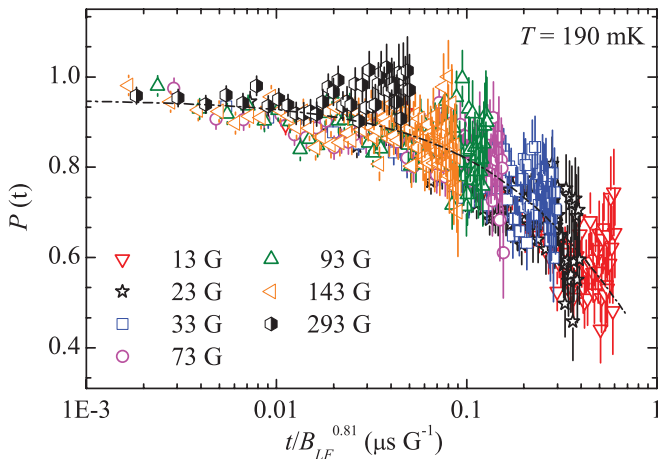
FIG. 4. (Color online) Corrected muon decay asymmetry at $T = 190$ mK for various magnetic fields as function of the scaling variable $t/B_{LF}^{0.81}$. The dashed-dotted line is a fit of the 13-G data with $P(t)/P(0) = \exp[-\lambda_L t]^{-0.9}$.

$P(t) = P(0)\exp[-(\lambda t)^\beta]$. An exponent of $\beta \approx 0.9$ shows that the relaxation rate is nearly uniform throughout the sample, indicating that YbNi$_4$P$_2$ exhibits quasihomogeneous spin fluctuations for $T \ll T_K$. The spin dynamics is characterized by a narrow distribution of correlation times ($\beta = 1$ corresponds to one single correlation time). Thus, disorder-driven theories, including Kondo disorder[25,26] and the Griffith phase scenario[27] as primary mechanisms for the observed NFL behavior, can be ruled out. It further implies that the crystalline disorder in YbNi$_4$P$_2$ is quite small, which is consistent with a small residual resistivity ($\rho_0 \sim 2.4 \, \mu\Omega$ cm) and the stoichiometric occupation of the crystallographic lattice sites revealed by the x-ray structure refinement.[12]

A sensitive test to identify power-law or stretched exponential behavior of $q(t)$ is a time-field scaling analysis of the muon-spin relaxation function. In both cases a specific time-field scaling can be found, i.e., the muon-spin relaxation function $P(t, B_{LF})$ obeys the scaling relation $P(t, B_{LF}) = P(t/B_{LF}^\gamma)$. This relation applies only in the asymptotic strong field limit, i.e., as long as $2\pi f_\mu = \gamma_\mu B_{LF} \gg \lambda_L$.[28] If time-field scaling is obeyed, a plot of $P(t, B_{LF})$ versus t/B_{LF}^γ at $T > T_C$ will

be universal for the correct choice of γ, and distinguishes between power-law ($\gamma < 1$) and stretched exponential ($\gamma \geqslant 1$) correlations. For small B_{LF}, the field dependence is expected to be due to the change of f_μ rather than an effect of field on $q(t)$. A breakdown of time-field scaling would occur for high fields where $q(t)$ is directly effected by the applied fields. Figure 4 shows the same asymmetry data, as displayed in Fig. 3, as functions of the scaling variable t/B_{LF}^γ. For $\gamma = 0.81(5)$ the data scale well over $\sim$2.5 orders of magnitude in t/B_{LF}^γ and for all fields between 13 and 143 G, except for 293 G. Here, at large t, the data fall above the low-field scaling curve. Fields $\mu_B B_{LF} \geqslant k_B T$ (with $k_B =$ Boltzmanns constant) would be expected to affect the spin dynamics. The scaling exponent $\gamma = 0.81(5) < 1$ implies that within the μSR frequency range, the spin-spin correlation function $q(t)$ is approximated by a power law (or a cutoff power law) rather than a stretched exponential or exponential,[28] consistent with the Redfield analysis. The power law is time-scale invariant and dynamical modulations should therefore be observable in any time window. The obtained time-field scaling of the relaxation data is a signature of slow homogeneous spin dynamics. It strongly indicates that the critical slowing down of spin fluctuations at the magnetic phase transition occurs cooperatively throughout the sample. In stoichiometric, homogeneous NFL systems such behavior may arise from the effect of disorder on quantum critical fluctuations inherent to a QCP. This is suggested for the NFL compound YbRh$_2$Si$_2$.[14,15]

In conclusion, ZF-μSR in the stoichiometric NFL compound YbNi$_4$P$_2$ clearly proves static magnetic ordering of strongly reduced Yb^{3+} moments below $T_C = 140$ mK. Above T_C, the muon-spin polarization $P(t)$ obeys the time-field scaling relation $P(t) = P(t/B^{0.81(5)})$ for applied magnetic fields B between 13 and 143 G, indicating cooperative and critical spin dynamics. Power-law behavior of the dynamic spin-spin autocorrelation function is implied by the observation of $\gamma < 1$.[28] The LF-μSR results suggest that the NFL behavior observed at $T > T_C$ is induced by quasihomogeneous critical spin fluctuations.

---

*h.klauss@physik.tu-dresden.de

[1] Focus issue on quantum phase transitions, Nat. Phys. **4**, 167 (2008).

[2] N. D. Mathur, F. M. Grosche, S. R. Julian, I. R. Walker, D. M. Freye, R. K. W. Haselwimmer, and G. G. Lonzarich, Nature (London) **394**, 39 (1998).

[3] G. R. Stewart, Rev. Mod. Phys. **73**, 797 (2001); **78**, 743 (2006).

[4] T. Park, F. Ronning, H. Q. Yuan, M. B. Salamon, R. Movshovich, J. L. Sarrao, and J. D. Thompson, Nature (London) **440**, 65 (2006).

[5] S. Friedemann, T. Westerkamp, M. Brando, N. Oeschler, S. Wirth, P. Gegenwart, C. Krellner, C. Geibel, and F. Steglich, Nat. Phys. **5**, 465 (2009).

[6] O. Stockert, J. Arndt, E. Faulhaber, C. Geibel, H. S. Jeevan, S. Kirchner, M. Loewenhaupt, K. Schmalzl, W. Schmidt, Q. Si, and F. Steglich, Nat. Phys. **7**, 119 (2011).

[7] T. R. Kirkpatrick and D. Belitz, Phys. Rev. B **67**, 024419 (2003).

[8] G. J. Conduit, A. G. Green, and B. D. Simons, Phys. Rev. Lett. **103**, 207201 (2009).

[9] S. J. Yamamoto and Q. Si, Proc. Natl. Acad. Sci. USA **107**, 15704 (2010).

[10] Una Karahasanovic, Frank Krüger, and Andrew G. Green, Phys. Rev. B **85**, 165111 (2012).

[11] R. Peters, N. Kawakami, and T. Pruschke, Phys. Rev. Lett. **108**, 086402 (2012).

[12] C. Krellner, S. Lausberg, A. Steppke, M. Brando, L. Pedrero, H. Pfau, S. Tencè, H. Rosner, F. Steglich, and C. Geibel, New J. Phys. **13**, 103014 (2011).

[13] D. E. MacLaughlin, O. O. Bernal, R. H. Heffner, G. J. Nieuwenhuys, M. S. Rose, J. E. Sonier, B. Andraka, R. Chau, and M. B. Maple, Phys. Rev. Lett. **87**, 066402 (2001).

[14] K. Ishida, D. E. MacLaughlin, B.-L. Young, K. Okamoto, Y. Kawasaki, Y. Kitaoka, G. J. Nieuwenhuys, R. H. Heffner, O. O. Bernal, W. Higemoto, A. Koda, R. Kadono, O. Trovarelli, C. Geibel, and F. Steglich, Phys. Rev. B **68**, 184401 (2003).

[15] D. E. MacLaughlin, R. H. Heffner, O. O. Bernal, K. Ishida, J. E. Sonier, G. J. Nieuwenhuys, M. B. Maple, and G. R. Stewart, J. Phys.: Condens. Matter **16**, 4470 (2004), and references therein.

[16] A. Schenck, *Muon Spin Rotation Spectroscopy: Principles and Applications in Solid State Physics* (Hilger, Bristol, 1985).

[17] S. G. Barsov *et al*., Hyperfine Interact. **64**, 415 (1990).

[18] E. I. Kornilov and V. Yu. Pomjakushin, Phys. Lett. A **153**, 364 (1991).

[19] R. S. Hayano, Y. J. Uemura, J. Imazato, N. Nishida, T. Yamazaki, and R. Kubo, Phys. Rev. B **20**, 850 (1979).

[20] A. Schenck, D. Andreica, F. N. Gygax, D. Aoki, and Y. Ōnuki, Phys. Rev. B **66**, 144404 (2002).

[21] A. Steppke (private communication).

[22] T. Moriya and T. Takimoto, J. Phys. Soc. Jpn. **64**, 960 (1995); A. Ishigaki and T. Moriya, *ibid*. **65**, 3402 (1996); T. Misawa, Y. Yamaji, and M. Imada, *ibid*. **78**, 084707 (2009).

[23] M. Sato, T. Hikihara, and T. Momoi, Phys. Rev. B **83**, 064405 (2011).

[24] J. S. Toll, Phys. Rev. **104**, 1760 (1956).

[25] E. Miranda, V. Dobrosavljevic, and G. Kotliar, J. Phys.: Condens. Matter **8**, 9871 (1996).

[26] E. Miranda, V. Dobrosavljevic, and G. Kotliar, Phys. Rev. Lett. **78**, 290 (1997).

[27] A. H. Castro Neto, G. Castilla, and B. A. Jones, Phys. Rev. Lett. **81**, 3531 (1998).

[28] A. Keren, P. Mendels, I. A. Campbell, and J. Lord, Phys. Rev. Lett. **77**, 1386 (1996).